Earth Planet. Sci. Lett. 674 (2026) 119741

Contents lists available at ScienceDirect

Earth and Planetary Science Letters

journal homepage: www.elsevier.com/locate/epsl

High-stress crystal plasticity of titanite and other minerals recording coseismic off-fault damage in strike-slip and thrust tectonic settings

Claudia A. Trepmann [a,*], Lisa M. Beiers [b], Fabian Dellefant [a,c]

[a] Ludwig-Maximilians-Universität München, Department of Earth and Environmental Sciences, Luisenstraße 37, D-80333 Munich, Germany
[b] Bochum University of Applied Sciences, Reservoir Geophysics, Am Hochschulcampus 1, D-44801 Bochum, Germany
[c] Ludwig-Maximilians-Universität München, Department of Cultural and Ancient Studies, Katharina-von-Bora-Str. 10, D-80333 Munich, Germany

ARTICLE INFO

Edited by\Dr A Webb

Keywords:
Mylonites
Pseudotachylytes
Silvretta basal thrust
Sesia zone
Twinned titanite
Stress

ABSTRACT

This study compares coseismic off-fault damage in a strike-slip (Sesia zone) and a thrust (Silvretta) tectonic setting to evaluate the different stress-strain histories. High-stress crystal plasticity at greenschist-facies conditions is recorded by mylonites from the Sesia zone and pseudotachylyte-bearing gneisses from the Silvretta basal thrust, European Alps. Twinned titanite occurring in both fault rocks highlights the similarities and differences in the recorded deformation. Fine-lamellar (< 1 μm) mechanical <110> twins in titanite from the Sesia mylonites with twin planes close to {221} show densities of 0.5 μm^{-1}. Consistent with twinned jadeite, the differential stresses indicated are on the order of 0.5 GPa. In the Silvretta fault rocks, the twin density is higher with 2.5 μm^{-1} and additionally, twin planes close to $\{\overline{1}12\}$ occur, indicating higher stress/strain-rate conditions, consistent with twinned amphibole and ilmenite as well as the presence of pseudotachylytes. The Silvretta fault rocks do not record subsequent creep, indicating rapidly decreasing stresses. In contrast, in the Sesia mylonites, subsequent creep of the surrounding quartz matrix at decreasing stresses resulted in sets of subparallel intragranular fractures in titanite, garnet, jadeite and zircon oriented at angles between 60° and 80° to the mylonitic foliation. The similarities of high-stress crystal plasticity in both settings with twinning at high differential stresses, as well as the differences with pseudotachylyte formation in the Silvretta fault rocks and creep at more slowly decreasing stresses in the Sesia zone mylonites, demonstrate the importance of deformation at transient high stresses for the subsequent stress-strain history.

1. Introduction

Stress-strain fields during seismic rupturing are known to be complex on all scales for all tectonic settings (e.g., Dielforder et al., 2023; Reches and Dewers, 2005; Scholz, 2002; Ulrich et al., 2019) with significant perturbations also below the seismogenic zone (e.g., Ellis et al., 2006; Ellis and Stöckhert, 2004; Nüchter and Ellis, 2011). At or just below the base of the continental seismogenic zone, i.e., at greenschist-facies conditions, crustal strengths and possible differential stresses reach a maximum dependent on the tectonic setting (e.g., Scholz, 2002). Yet, as these depths are not directly accessible to us for *in situ* measurements, little is known about the different stress-strain histories and the deformation behavior of rocks in different tectonic settings during the seismic cycle. A low gradient in temperature and pressure can be expected in thrust settings, given the low dip angle of the fault plane, as well as for strike-slip faults with low vertical offset. In contrast, the significant vertical offset in normal fault settings causes marked gradients in temperature-pressure conditions during faulting (e.g., Scholz, 2002). Therefore, fault rocks from strike-slip and thrust tectonic settings are especially suitable to record differences in the stress-strain history during episodic deformation, where the influence of temperature change during faulting is comparatively small. Here, we use the record of mylonites from the tectonic strike-slip setting of the Insubric Fault System of the Sesia zone and of pseudotachylyte-bearing gneisses from the Silvretta basal thrust fault, both deformed at greenschist facies conditions (Sesia: Stöckhert et al., 1986; Zucali et al., 2002; Silvretta: e.g., Brückner et al., 2023; Koch and Masch, 1992; Maggetti and Flisch, 1993), to compare and contrast the deformation behavior in the two different tectonic settings. Twinned titanite occurs in both fault rocks and highlights the similarities and differences of the stress-strain history and shows its interplay with rock-forming and other accessory minerals during episodic deformation at transient stresses.

Microstructures from fault rocks exhumed in tectonically active

* Corresponding author.
E-mail address: claudia.trepmann@lmu.de (C.A. Trepmann).

https://doi.org/10.1016/j.epsl.2025.119741
Received 27 April 2025; Received in revised form 9 November 2025; Accepted 15 November 2025
Available online 26 November 2025

regions have been proven to be valuable in recording the stress-strain history at depths of the continental seismogenic zone, i.e., at greenschist-facies conditions (e.g., Anderson et al., 2021; Brückner and Trepmann, 2021; Küster and Stöckhert, 1999; Trepmann and Stöckhert, 2003, 2001), as well as at even greater depths of mid to lower crustal conditions (e.g., Austrheim et al., 2017; Campbell and Menegon, 2022; Toffol et al., 2024). Episodic deformation at transient high stresses related to the seismic cycle has been found in these studies to be dominated by dislocation glide, twinning and kinking, associated with cataclasis. This deformation behavior is known as high-stress crystal plasticity (or low-temperature plasticity, power law breakdown, Peierls creep), where, in contrast to dislocation creep, dislocation climb and thus recovery is not efficient given the higher stresses and strain rates (e.g., Frost and Ashby, 1982; Kameyama et al., 1999; Tsenn and Carter, 1987). The stored strain energy introduced during high-stress crystal plasticity can lead to enhanced creep at decreasing stresses after high-stress deformation in the affected volumes. This results in specific modifications of the high-stress microstructures as documented from the natural rock record in combination with deformation experiments (e.g., Trepmann et al., 2007; Trepmann and Stöckhert, 2003). Commonly, pseudotachylytes are assumed to be the only microstructural evidence indicating deformation related to the seismic cycle (e.g., Anderson et al., 2021; Sibson, 1975). The record of mylonites on transient deformation episodes at high stresses is still underestimated, which is partly due to the subsequent creep at less rapidly decreasing stresses, obscuring the high-stress event. However, the recognition and consideration of deformation episodes at transiently high stresses below the seismogenic zone - instead of assuming long-term deformation at stationary stress-strain conditions – is relevant for example for understanding the stress build-up within the seismogenic zone (e.g., the "deep slip model" of Scholz, 2002), as well as understanding the energy budget of earthquakes (Anderson et al., 2021).

Especially mechanical twins (or *deformation twins*, e.g., Christian and Mahajan 1995) that require a high critical resolved shear stress (CRSS), such as jadeite (150 MPa; Orzol et al., 2003) and amphibole (200–400 MPa, Rooney et al., 1970), are valuable indicators of transient high stresses in fault rocks (e.g., Brückner and Trepmann, 2021; Campbell and Menegon, 2022; Trepmann and Stöckhert, 2001). As twin boundaries are characterized by low interfacial free energy, they are relatively stable during subsequent modification at lower stresses during the prolonged geological history before exhumation from the base of the seismogenic zone. Mechanical twins are also known as shock effects at moderate shock conditions (shock pressures of 7–30 GPa) during hypervelocity impact (e.g., Dellefant et al., 2022 (ilmenite and magnetite); Dellefant et al., 2024a (amphibole); Poelchau et al., 2025 (calcite); Seybold et al., 2023 (calcite); Stöffler et al., 2018, and references therein). Twinned titanite has been reported from impact breccias (McGregor et al., 2021; Papapavlou et al., 2018; Timms et al., 2019), nuclear tests (Borg, 1970) and deformation experiments (Borg and Heard, 1972), where the CRSS for ⟨110⟩ twins has been constrained to 130 MPa. So far, deformed titanite has rarely been described in detail from fault rocks, although it is an important mineral that can constrain the time of deformation by U-Pb dating (Bonamici et al., 2015; Corvò et al., 2023; Müller and Franz, 2004). Whether the U-Pb concentration is modified by the deformation of titanite is linked to how much diffusion and local interaction of titanite with fluids are involved during and/or after deformation (Corvò et al., 2023). The thorough characterization of titanite microstructures in relationship to those of other minerals in different geological settings may contribute to evaluating the geochronological record of titanite in fault rocks (Bonamici et al., 2015; Corvò et al., 2023) as well as in impact structures (Papapavlou et al., 2018). Generally, the significant similarities of high-stress crystal plasticity during faulting and hypervelocity impact, where likewise high differential stresses on the order of GPa occur, are associated with moderate shock conditions (shock pressures on the order of 10 s of GPa, e.g., Rae et al., 2021; Trepmann, 2008). Therefore, we compare our findings to the record of impact breccias. The comparison of high-stress plasticity in different geological settings contributes to a better knowledge of the distribution and importance of episodic deformation at transient high stresses in nature.

2. Methods

The microfabrics were analyzed using polished thin sections with approximately 25 μm thickness. The thin sections of the mylonites were cut perpendicular to the macroscopic foliation and parallel to the stretching lineation (xz cuts, Fig. 1a–c). The pseudotachylyte-bearing gneisses were cut perpendicular to the foliation of the gneisses, which contain μm- to mm-scaled irregular pseudotachylytic veins that crosscut the main foliation at varying angles (Fig. 1d–f). For scanning electron microscopy (SEM), we used a field emission Hitachi SU5000 microscope, equipped with a NordlysNano (Oxford Instruments) high-sensitivity electron backscatter diffraction (EBSD) detector and energy dispersive spectrometer (EDS, Oxford Instruments). For EBSD analysis, the samples were mechano-chemically polished using a highly alkaline colloidal silicon suspension. For acquiring the EDS and EBSD signals, AZtec 6.0 analysis software (Oxford Instruments) was used. The SEM was operated at accelerating voltages of 10–20 kV and a working distance of 10 mm (for EDS measurements) and 20–25 mm (for EBSD measurements). The step size for automatic EBSD mapping using a sample holder pre-tilted at 70° with respect to the electron beam was in the range of 0.5–1 μm, depending on the EBSD pattern quality and required resolution. The EBSD data were processed using the AZtecCrystal 3.0 software (Oxford Instruments). Single pixels that are different from the surrounding pixels sharing a common but different orientation were automatically replaced with the orientation extrapolated from the surrounding orientations. Non-indexed points were replaced by the average orientation of six surrounding pixels. EBSD is used to analyze different crystallographic orientations by determining the lowest angle that allows one orientation to be rotated into another, i.e., the disorientation angle and the disorientation axis. Twin boundaries are defined by the crystallographically controlled misorientation angle and misorientation axis with a maximum deviation angle of 5° Grains are detected by a misorientation angle threshold of 10° These settings were double-checked by comparing the resulting orientation maps with the band contrast map to avoid artefacts. All pole figures are stereographic projections of the lower hemisphere. The EBSD maps are presented using the Inverse Pole Figure (IPF) color code to show the orientation of grains with respect to the sample reference frame. To quantify the misorientation within one grain, the Grain Reference Orientation Deviation (GROD) angle is used, which is the misorientation angle between the orientation at a pixel and the mean orientation of the grain.

3. Geological overview and samples

Deformed titanite [$CaTi(SiO_4)O$] is abundant in mylonites from the Sesia zone in the Western European Alps (Fig. 1a–c) and pseudotachylyte-bearing amphibole-rich gneisses in the damage zone of the Silvretta basal thrust in the Central European Alps (Fig. 1d–f). We chose characteristic samples of each locality for comparison.

3.1. Mylonites from the Sesia zone

The mylonite from the Sesia zone was sampled close to the village of Montestrutto (45°32′22.10″N; 7°50′19.77″E; CT183) from the Ivozio complex, which is part of the Eclogitic Micaschists Complex of the Austroalpine Sesia-Lanzo Zone (Zucali and Spalla, 2011). During Alpine orogeny, the Ivozio complex experienced an early Alpine eclogite-facies overprint. Subsequent retrogression at greenschist-facies conditions at 300–350 °C and relatively high pressures of possibly 700–800 MPa is indicated by phengite formed from retrogression of jadeite (Stöckhert et al.,

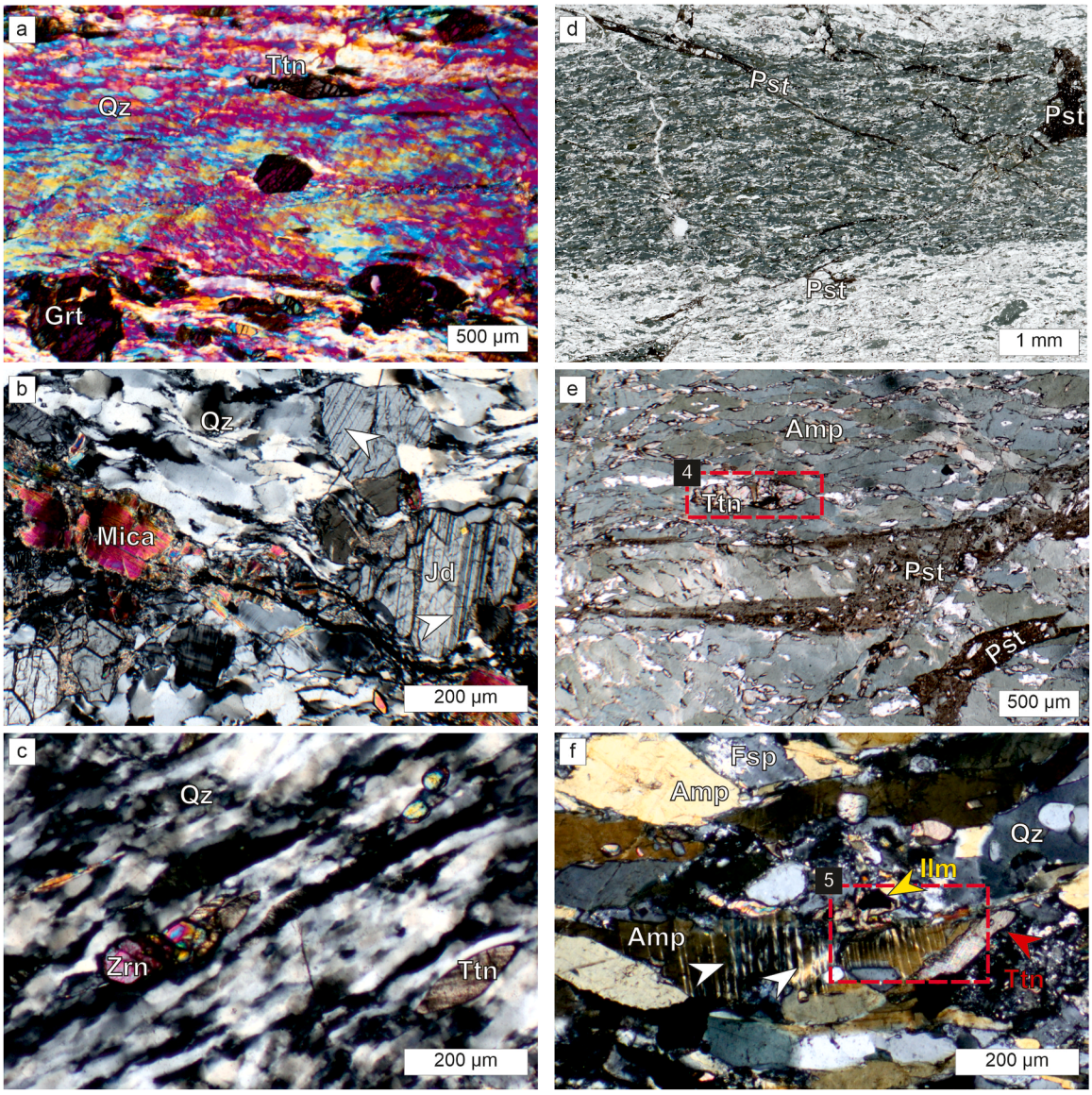

Fig. 1. Polarized light micrographs of microstructures indicating high-stress crystal plasticity. (a-c) Sesia mylonite CT183 showing cataclastically deformed titanite (Ttn), garnet (Grt), jadeite (Jd) and zircon (Zrn) in a quartz (Qz) matrix. White arrows in (b) indicate (100)<001> twins in jadeite; (a-c) are taken with crossed polarizers, in (a) the compensator plate is inserted. (d, e) Pseudotachylyte (Pst)-bearing fault rock from the damage zone of the Silvretta basal thrust, sample LB21b. Rectangle in (e) marks titanite analyzed by EBSD displayed in Fig. 4. (f) Pseudotachylyte-bearing Silvretta fault rock, sample LB22a (crossed polarizers). Amphibole with $(\bar{1}01)[101]$ twins, marked by white arrows, occurs associated with twinned titanite (Ttn; red arrow) and twinned ilmenite (Ilm; yellow arrow). The rectangle marks the EBSD map shown in Fig. 5.

1986; Zucali et al., 2002). At these conditions, the mylonites formed from eclogite-facies, jadeite-bearing metagranites. They contain quartz (ca. 65 %), garnet (ca. 10 %, $Fe_{1.5–1.3}Ca_{1.4–1.2}Mg_{0.2}Mn_{0.1}Al_2Si_3O_{12}$), phengite (ca. 15 %), jadeite (ca. 5–10 %, $Na_{0.95–0.92}Ca_{0.2}Mg_{0.2}Fe_{0.2–0.1}Al_{0.9–0.8}Si_2O_6$), as well as accessory titanite, zircon, rutile and apatite (Figs. 1a-c, S1). The mylonite is characterized by a partially recrystallized quartz microfabric forming a mylonitic foliation (Fig. 1b, c; Trepmann and Stöckhert, 2003). The orientation distribution of (100)[001] twins in jadeite (Fig. 1b) with a CRSS of 150±25 MPa (Orzol et al., 2003) indicates differential stresses on the order of 0.5 GPa during deformation (Trepmann and Stöckhert, 2001). The episodic deformation at transient high stresses at greenschist facies conditions has been associated with seismic rupturing in the formerly overlying upper crust (Küster and Stöckhert, 1999; Trepmann and Stöckhert, 2003, 2002, 2001). The seismic rupturing is likely related to a precursor fault of the Insubric strike-slip fault system, a western part of the Periadriatic fault system (Schmid et al., 2004, 1989).

3.2. *Pseudotachylyte-bearing amphibole-rich gneisses from the Silvretta nappe*

The pseudotachylyte-bearing amphibole-rich gneisses from the damage zone of the Silvretta basal thrust were sampled close to the Wiesbadener hut in the Ochsental (46°51′55″ N / 10°07′03″ E, LB21, 22), laterally >2 km from the contact to the underlying Penninic units. They contain alternating feldspar-quartz-rich layers and amphibole-rich layers (Fig. 1d). The latter can contain >80 % amphibole [green hornblende, $(Na, K)_{0.3–0.6}(Ca, Mn)_2(Mg_{2.2}Fe_{1.8}Al)(Si_7Al)O_{22}(OH)_2$] and abundant titanite (Fig. 1d–f).

The Silvretta nappe represents one of the Upper Austroalpine basement nappes, covers about 1600 km^2 and is mainly composed of polymetamorphic paragneisses, orthogneisses, and amphibolites (Maggetti and Flisch, 1993; Thöni, 1988). The pseudotachylytes occur in an area of at least 100 km^2 and up to 500–900 m above today's contact with the overthrusted Penninic units (Schmutz, 1995). They can be concordant or

discordant to the pre-Alpine foliation of the gneisses (Schmutz, 1995). The pseudotachylytes formed about 75 Ma ago (Ar/Ar and Rb/Sr isotopic investigations; Bachmann et al., 2009; Thöni, 1988) during the detachment of the Silvretta nappe from its original substratum (Insubric crystalline; Koch and Masch, 1992; Laubscher, 1983; Schmutz, 1995). During nappe transport, no marked strain was accumulated in the Silvretta nappe, but strain largely accumulated in the underlying Penninic units (Laubscher, 1983). Greenschist-facies conditions with temperatures at about 350 ± 50 °C and pressures of about 200–400 MPa during pseudotachylyte formation are constrained by the occurrence of stilpnomelane-epidote mineral assemblage (e.g., Brückner et al., 2023; Koch and Masch, 1992; Maggetti and Flisch, 1993). Recently, Pittarello et al. (2022) suggested that pristine pseudotachylytes with skeletal intergrowth of plagioclase-amphibole aggregates formed at temperatures <250 °C. Yet, Koch and Masch (1992) as well as Brückner et al. (2023) reported that stilpnomelane can also be present in otherwise pristine pseudotachylytes with skeletal intergrowth of plagioclase-amphibole aggregates indicating greenschist facies conditions, which is consistent with associated quartz microfabrics (e.g., Bachmann et al., 2009; Brückner et al., 2023; 2024; Trepmann et al.,

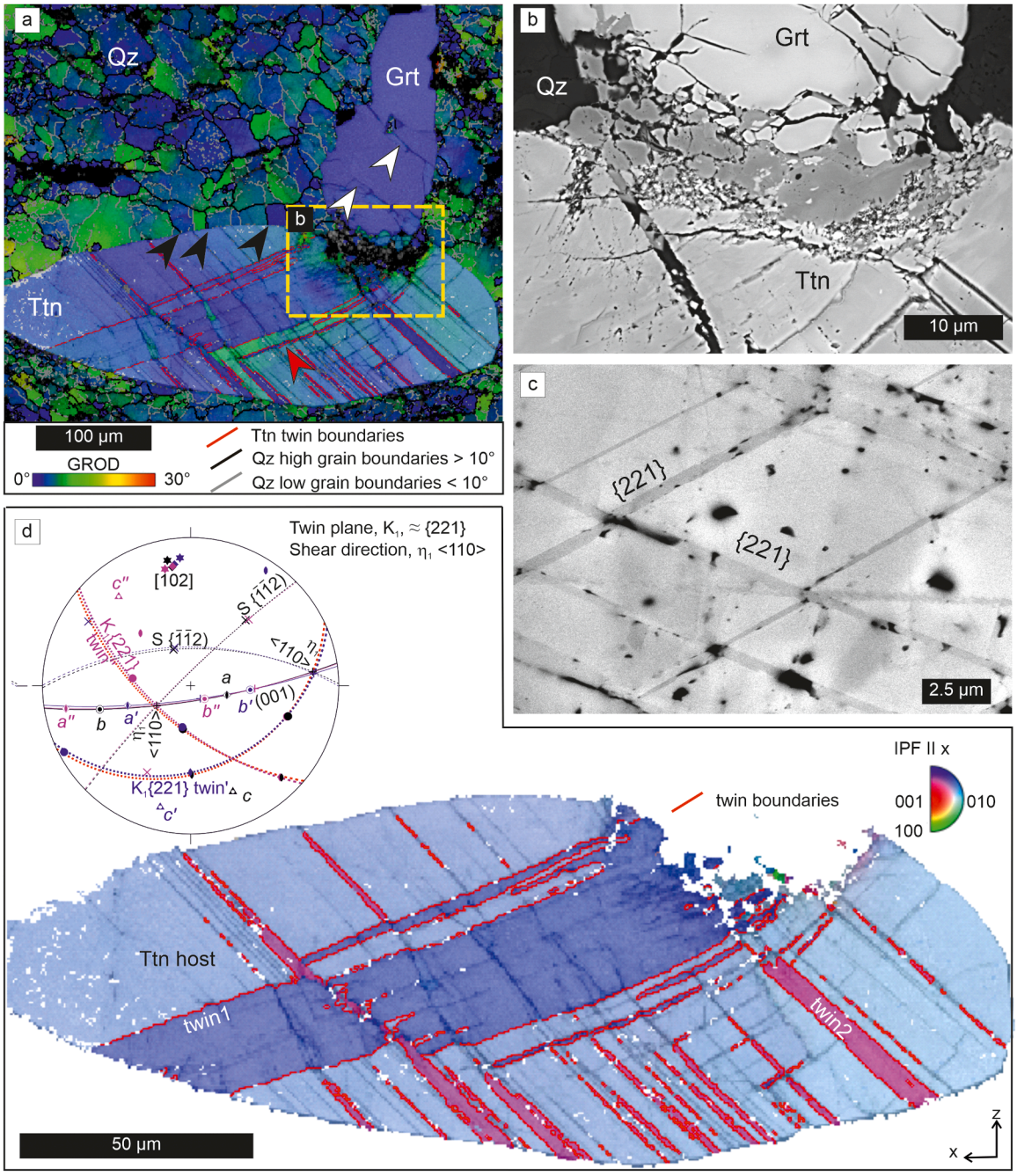

Fig. 2. SEM data of twinned titanite (Ttn) with brittle contact zone to garnet (Grt) in a quartz (Qz)-rich matrix, Sesia mylonite sample CT183. (a) GROD angle map. Black arrows point to quartz grain boundaries at a high angle to the titanite phase boundary. White arrows indicate fractures in garnet. Red arrow points to bent twins. (b) BSE image of brittle contact between garnet and titanite, location shown in (a). (c) BSE image displaying the orientation contrast of thin twin lamellae in titanite. (d) IPF close-up map of twinned titanite, reference direction is the horizontal line X, corresponding to the macroscopic lineation of the mylonite. Twin boundaries are indicated by red lines. Stereographic projection depicts the orientation relation of the two twin domains to the host titanite, see text for explanation. The colors refer to the IPF map.

2017). Amphibole in the pseudotachylyte-bearing gneisses contains ($\bar{1}01$) twins (Fig. 1d), which require a CRSS of 200–400 MPa (Rooney et al., 1970), indicating differential stresses of >400 MPa during deformation (Brückner and Trepmann, 2021).

4. Results

4.1. Titanite high-stress crystal plasticity in the Sesia mylonites

Twinned and cataclastically deformed titanite is associated with cataclastically deformed zircon, garnet and jadeite (Fig. 1a–c, Fig. S1a). In addition to titanite, also jadeite (Fig. 1b) and rutile (Fig. S1b, c) are twinned. Titanite twins (Fig. 2) are characterized by EBSD by a disorientation angle of 74° to the host and a disorientation axis (da) of [102]. This twinning can be described by a 180° rotation about ⟨110⟩, which is the shear direction, η_1. The twin and composition plane, K_1, is close to {221} (Fig. 2d; Borg, 1970; Timms et al., 2019). The plane of shear, defined by the pole to {221} and the shear direction ⟨110⟩ is {$\bar{1}\bar{1}$2}. Another common plane of the twin and the host is (001). The common directions and planes in twin and host are identified by EBSD measurements (Fig. 2d). The twins in titanite can be <1 μm narrow with a spacing of as low as 1 μm to several tens of μm and a varying twin density of up to 0.5 μm^{-1} (number of lamellae per unit length) measured in BSE images (Fig. 2c). Commonly two symmetrically equivalent twin domains occur, where the twin planes are close to the two symmetrically equivalent {221} planes (Fig. 2a, c, d, Fig. S1a). About 20 % of the titanite crystals in the studied samples do not show twins, about 45 % show one twin set and about 35 % two twin sets. The angle of the twin planes to the foliation varies from 2° to 89° with a maximum of 15° for the one twin set and 44° for the second twin set. No systematic dependence of the twin density on grain size has been detected.

Brittle deformation can be concentrated where garnet (Fig. 2,

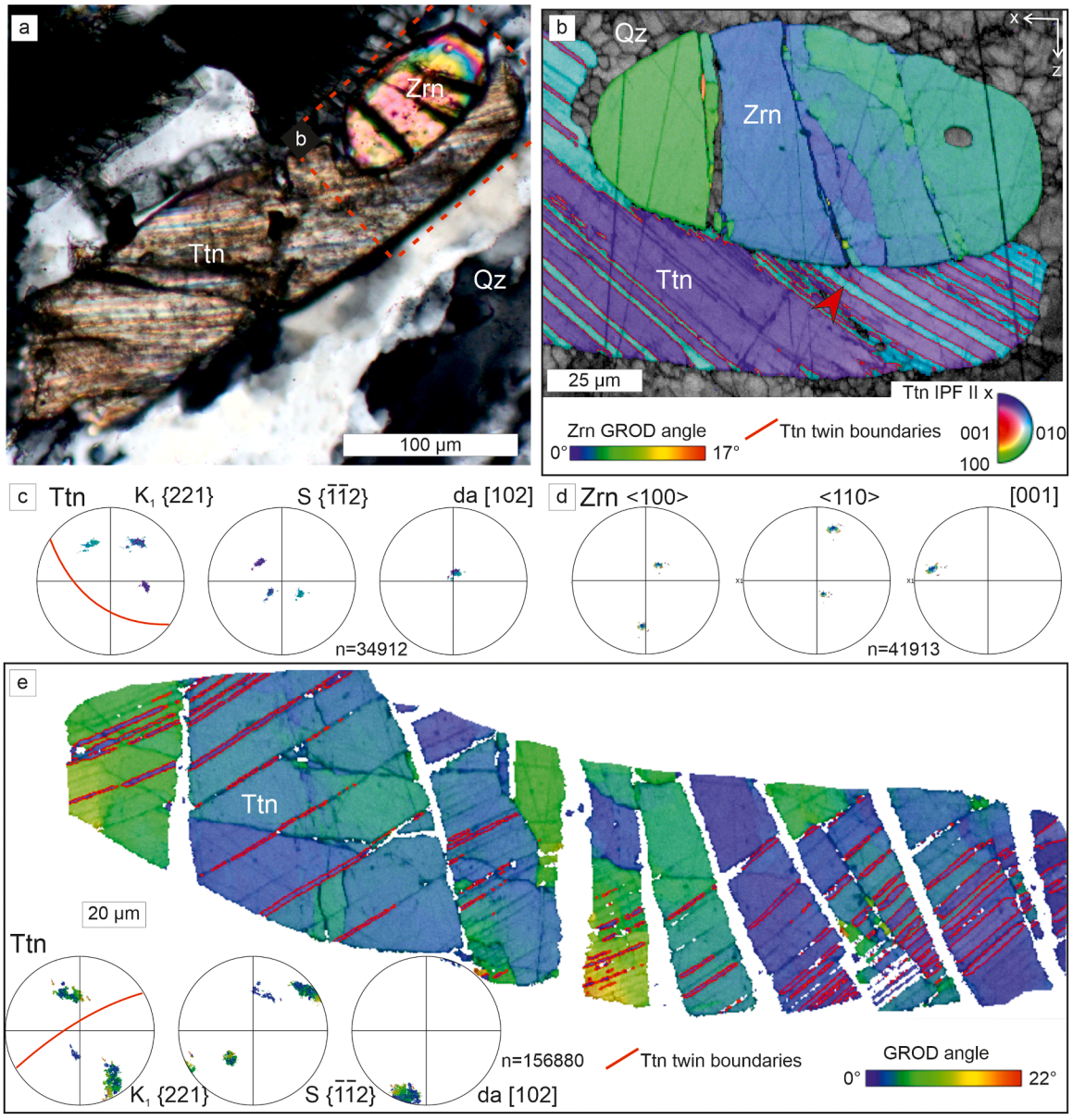

Fig. 3. Deformed zircon (Zrn) and titanite (Ttn), Sesia mylonite sample CT183. (a) Polarized light micrograph (crossed polarizers) displaying zircon indenting in twinned titanite. Red rectangle marks the location of EBSD map shown in (b). (b) IPF map of twinned titanite, reference direction is the horizontal line X, corresponding to the macroscopic lineation of the mylonites, and GROD angle of zircon. Twin boundaries in titanite are indicated by red lines. Red arrow indicates bent twins. (c, d) Stereographic projection of the corresponding crystallographic orientation of titanite and zircon, respectively. (e) Stereographic projection and GROD angle map of cataclastically deformed twinned titanite. Twin boundaries are indicated in red.

Fig. S1a) or zircon (Figs. 1a, c, 3, 4) indent into titanite. Garnet has microcracks and typically a low internal misorientation (Fig. 2a, Fig. S1c). The garnet is Fe- and Ca-rich ($Fe_{1.5}Ca_1Mg_{0.3}Mn_{0.2}Al_2Si_3O_{12}$). The fragmented zone between garnet and titanite (medium grey in Fig. 1b) is enriched in Ca and Ti and depleted in Fe, Mg, and Mn, while Al and Si are relatively stable compared to garnet. Relative to titanite [$CaTi(SiO_4)O$], the zone is enriched in Al and Fe and depleted in Ti and, to a lesser extent, in Ca. Otherwise, there is no chemical variance in the deformed garnet or titanite associated with the deformation microstructures. Titanite has an internal misorientation with GROD angles typically <15° and up to 20° (Figs. 2a, 3e). The twin boundaries can be slightly bent towards indenting garnet or zircon (red arrows in Figs. 2a, 3b). In zircon, low GROD angles of <10° are mostly related to microfractures (Fig. 3b). The occurrence or density of twins in titanite is not dependent on or restricted to these zones of localized brittle deformation (Fig. 3a, e).

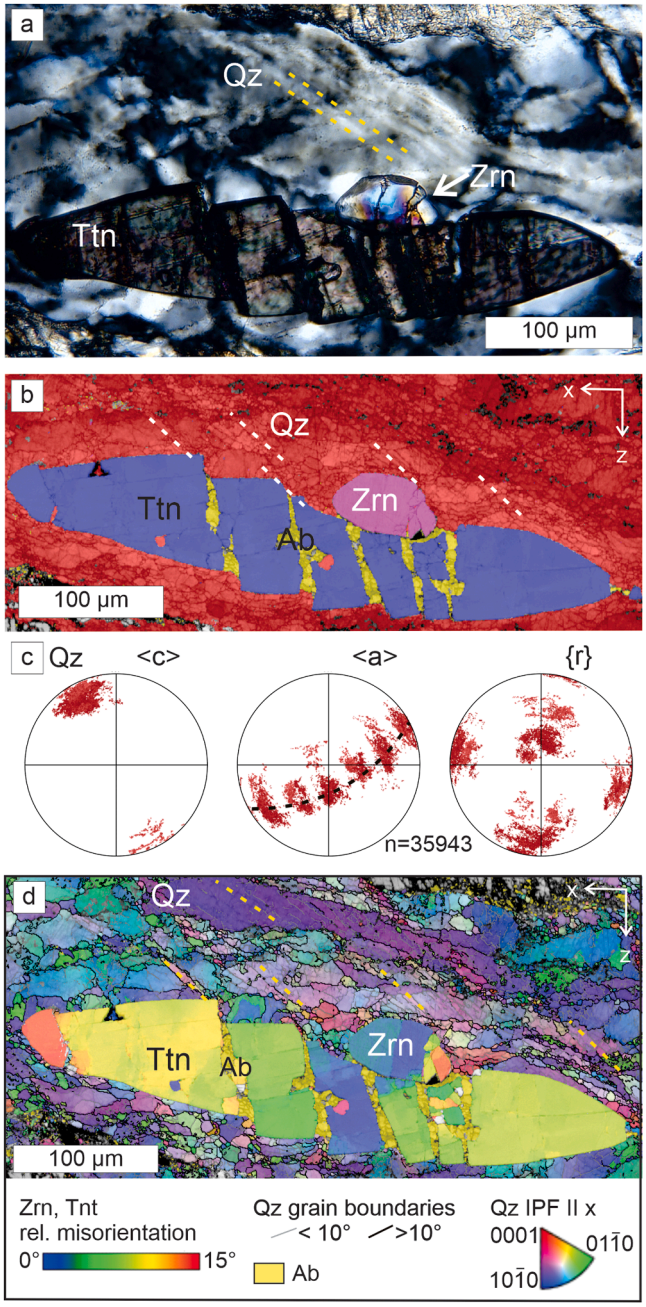

Fig. 4. Cataclastically deformed titanite (sample CT183). (a) Polarized light micrograph (crossed polarizers) showing zircon (Zrn) indenting in cataclastically deformed titanite (Ttn) surrounded by quartz (Qz) and (b) corresponding EBSD phase map: quartz (Qz, red), titanite (Ttn, blue), zircon (Zrn, pink) and albite (Ab, yellow). Note the subbasal deformation lamellae marked by white dashed lines. (c) Polefigure of quartz *c*-, *a*-axes and poles to *r*-planes of quartz grains containing subbasal deformation lamellae (black dashed line). (d) Same EBSD map as in (b) with Inverse Pole Figure (IPF) color coding for quartz, albite as phase (yellow) and relative misorientation for titanite and zircon.

Fragments in cataclastically deformed titanite are separated by few µm (up to 20 µm, Figs. 3e, 4a, b, d), where the space in-between is filled by quartz or albite (yellow in Fig. 4b). The spacing of the fragments does not systematically vary with the spacing of the fractures nor with the angle to the mylonitic foliation. The rotation of the fragments appears relatively minor (Figs. 3e, 4). The twin lamellae can be followed continuously over separated fragments, indicating that twinning occurred before cataclasis (Fig. 3e).

At the phase boundary to twinned titanite, quartz has grain boundaries at high angle to the interphase (black arrows in Fig. 2a). Subbasal deformation lamellae in quartz enclose an angle of 40–50° to the mylonitic foliation (Fig. 4). These observations suggest that dislocation glide-controlled deformation of quartz can be localized at the contact to twinned titanite. The quartz microstructures characterized here and in other mylonites from the Sesia zone developed through initial dislocation-glide controlled deformation at high differential stress with subsequent creep at decreasing stresses (Trepmann and Stöckhert, 2003).

4.2. *Titanite high-stress crystal plasticity in the Silvretta pseudotachylyte-bearing gneisses*

Titanite in the pseudotachylyte-bearing Silvretta gneisses (Figs. 1e–f, 5, 6) that occur related to the basal thrust up to 500–900 m above todays contact to the Penninic units has similar twins as those in the Sesia mylonites (Figs. 2, 3, Fig. S2). The twins are characterized by a disorientation axis of [102] and a disorientation angle of 74° (Figs. 5, 6). Also here, two sets approximately parallel to both symmetrically equivalent {221} planes occur (Figs. 5, 6, Fig. S2). Additionally, titanite can contain domains with misorientation angles < 10° with subparallel boundaries following {010}, and <100> rotation axis, suggesting {001}<010> glide (Fig. 5b, c). The sharp but slightly irregular boundaries that deflect the twins resemble kink bands. Furthermore, twins with the same disorientation axis [102] and disorientation angle of 74° can display twin boundaries subparallel to a common $\{\bar{1}\bar{1}2\}$ plane (Fig. 6b), which has, to our knowledge, not been described before. Twin densities vary and are with of up to 2.5 μm^{-1} (lamellae per unit length) measured in BSE images (Fig. 6, Fig. S2a) higher than those observed in the Sesia mylonites. About 7 % of the titanite observed do not show twins, about 55 % of the titanites show one twin set and about 38 % two twin sets. The angle of the twin planes to the foliation of the gneisses varies from 3° to 76° to the foliation with a maximum of 18° for the one twin set and 46° for the second twin set. Associated with twinned titanite, twinned amphibole and twinned ilmenite occur (Fig. 6a, Fig. S2b). The amphibole twins are parallel $(\bar{1}01)$ and show disorientation axes of [101] and a disorientation angle of 180°, as described by Brückner and Trepmann (2021). The ilmenite twins are fine-lamellar with boundaries parallel to $\{10\bar{1}1\}$ and characterized by a disorientation axis $< 1\bar{1}0\bar{1} >$ and disorientation angle of approximately 69° Similar twins have been reported from gneisses of the Vredefort impact structure (Dellefant et al., 2022). Moreover, the occurrence of ilmenite twins parallel $\{10\bar{1}1\}$ is reported from lunar rocks and shock experiments (Minkin and Chao, 1971; Sclar et al., 1973). Titanite inclusions in twinned amphibole show misoriented domains at the contact to the amphibole twins (white arrows in Fig. 7), where likewise the amphibole twins show internal misorientations (black arrows in Fig. 7).

Twinned titanite appears to occur independently of the distance to single µm- to mm-scaled pseudotachylytic veins, which are crosscutting

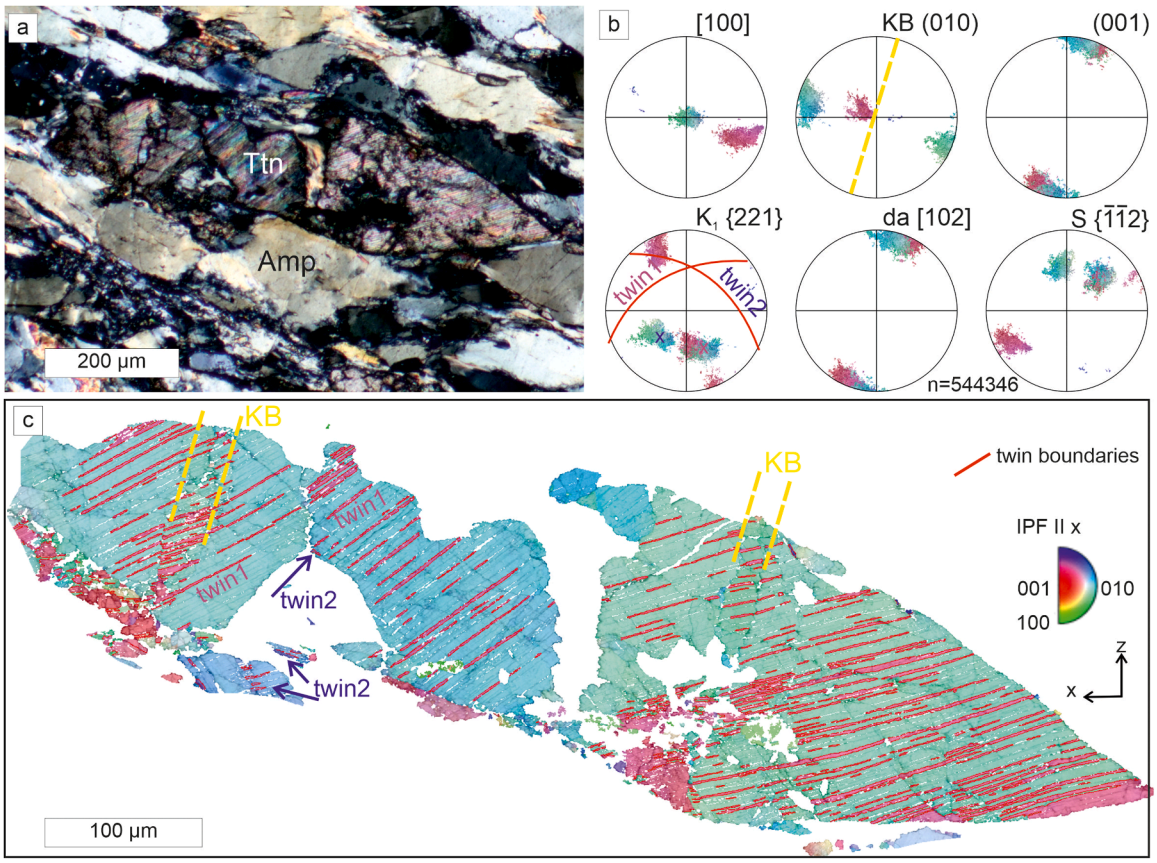

Fig. 5. Twinned titanite in Silvretta pseudotachylyte-bearing fault rock, sample LB21. (a) Polarized light micrograph (crossed polarizers) of twinned titanite (Ttn) and amphibole (Amp). (b, c) EBSD data of deformed titanite with pole figures and corresponding IPF map with kink bands (KB, yellow dashed lines), reference direction is the macroscopic lineation of the gneiss. Twin boundaries are indicated by red lines.

the foliation in the gneisses at varying angles (Fig. 1d–f). At the direct contact to pseudotachylytic veins, titanite shows in BSE images grey scale orientation contrasts indicating enhanced relative misorientations and very thin (<1 µm) twin lamellae that are deflected just adjacent to the pseudotachylytic veins (Fig. 8a–c). EBSD measurements (Fig. 8b) confirm the indicated misorientation by increased GROD angles of up to 15° and the presence of twins with [102] disorientation axes and a disorientation angle of 74°. Yet, the resolution of the EBSD data does not allow further quantification, as the index rate of the titanite just adjacent to the pseudotachylytic vein can be reduced (compare white arrows in Fig. 8b, c), indicating high misorientations and high defect densities. Brittle deformation of titanite (Fig. 8d, e), as well as of other minerals such as apatite (Fig. 8e) and zircon (Fig. 8f), resulted in more or less isometric clasts with low aspect ratios. This is in marked contrast to the Sesia zone mylonites, where sets of subparallel fractures at 60–80° to the mylonitic foliation are dominating in all rock-forming minerals (compare Fig. 8 and Figs. 1a–c, 3).The surrounding matrix of coarse-grained feldspar and quartz grains, as well as adjacent quartz-rich, pseudotachylyte-bearing layers, shows no evidence of creep associated with twinned titanite (Fig. 1d–f, Fig. S2a). These observations are consistent with missing strain gradients of the quartz matrix associated with twinned amphibole or pseudotachylytes recorded by Brückner and Trepmann (2021) and Brückner et al. (2023).

5. Discussion

The deformation described here, represents the off-fault damage in a large volume at some distance from the main rupture. In the Silvretta, the hanging wall is preserved, and the thrust is represented today by the contact to the Penninic units (e.g., Koch and Masch, 1992; Schmutz, 1995). In the Sesia zone, the deformation is most probably related to the activity of a precursor fault of the Insubric fault system, which did not propagate down into the depth level of the presently exposed Sesia zone (Küster and Stöckhert, 1999; Trepmann and Stöckhert, 2003). Temperature conditions during deformation are for both tectonic settings constrained to 350 ± 50 °C (Fig. 9, e.g., Silvretta: Brückner et al., 2023; Koch and Masch, 1992; Sesia: Stöckhert et al., 1986; Zucali et al., 2002). Whereas mechanical twinning of rock-forming minerals indicates high differential stresses for both tectonic settings, there are also major differences, which include the fracture pattern of accessory minerals and the different behavior during the subsequent stage at lower stresses (Table 1), which are discussed in the following.

5.1. Mechanical twins indicate transient peak stresses

Mechanical twinning is a dislocation glide-controlled plastic deformation mechanism, where the nucleation and growth of twins (in length and thickness) are facilitated by the generation and glide of dislocations, requiring a CRSS on the specific twin planes in the shear direction (e.g., Christian and Mahajan 1995). Titanite twins with a disorientation axis of [102] and disorientation angle of 74° and a glide direction of <110> have been described from terrestrial impact breccias (McGregor et al., 2021; Papapavlou et al., 2018; Timms et al., 2019), nuclear tests (Borg, 1970) and deformation experiments, which constrained a CRSS of ca. 130 MPa (Borg and Heard, 1972). To our best knowledge, it is the first time that titanite twins characterized by a disorientation axis of [102], a disorientation angle of 74°, with ⟨110⟩ glide directions and various twin planes parallel ≈{221} and ≈{$\bar{1}\bar{1}$2} (Fig. 6a–d) have been described from greenschist-facies fault rocks. Müller and Franz (2004) described "unusual deformation microstructures in garnet, titanite and clinozoisite

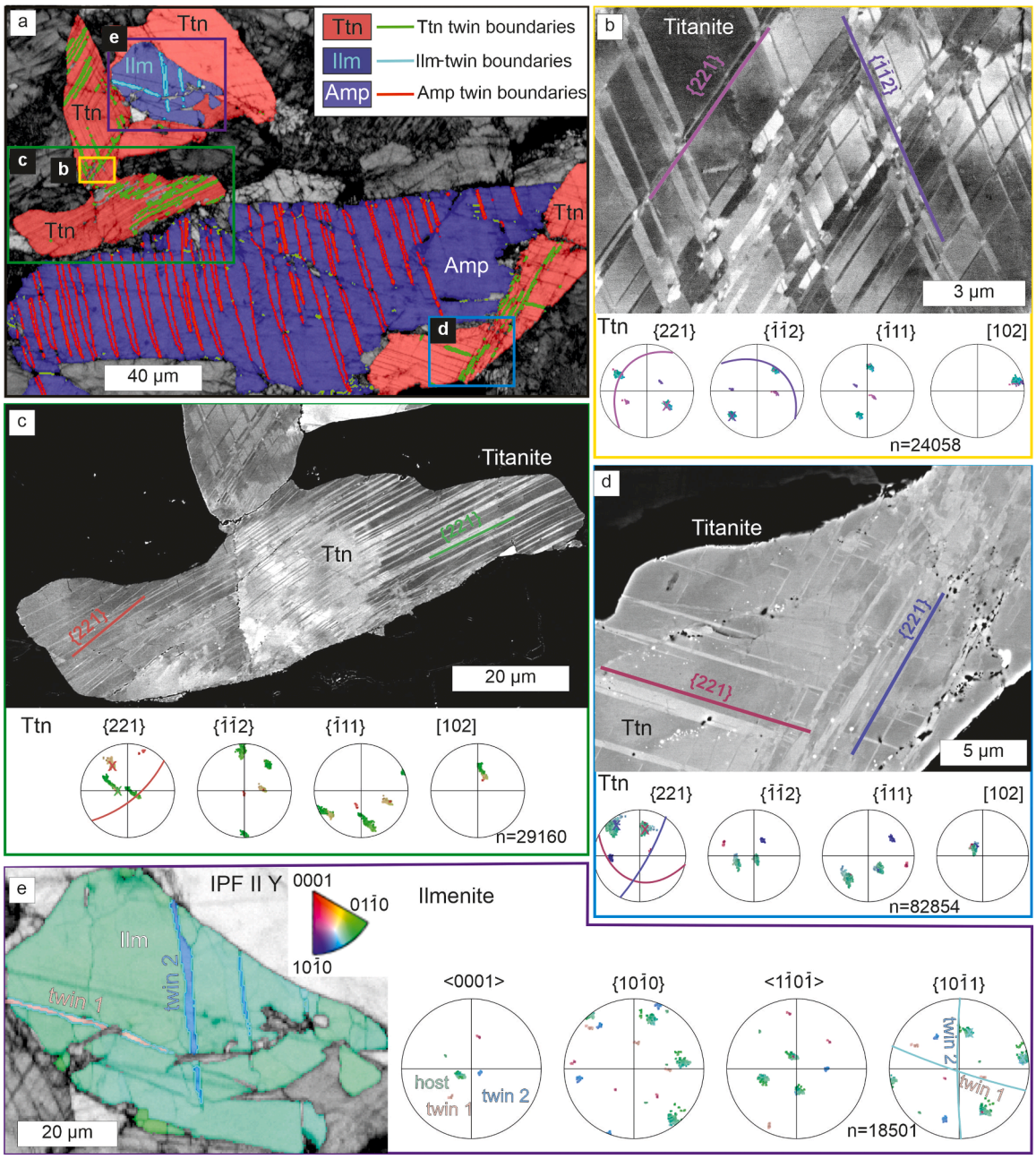

Fig. 6. Twinned titanite, amphibole and ilmenite in Silvretta pseudotachylyte-bearing fault rock, sample LB22. (a) EBSD phase map showing twinned titanite (red, Ttn), twinned amphibole (blue, Amp) and twinned ilmenite (purple, Ilm), with twin boundaries indicated by green, red and turquoise colors, respectively. (b-d) BSE images and pole figures for grains, as indicated in (a). (e) IPF color-coded ilmenite EBSD map with corresponding pole figures showing two symmetrically equivalent $\{10\bar{1}1\}$ twins in ilmenite.

from an eclogite of the Lower Schist Cover, Tauern Window, Austria". They performed TEM investigations of crystal-plastically deformed titanite that revealed Burgers vectors of free dislocations with $b = [100]$, dislocations of low-angle grain boundaries with $b = [011]$ and locally twin lamellae. However, the twin system was not further specified. Twinned and crystal-plastically deformed titanite has been used to constrain the time of deformation at granulite- and amphibolite-facies conditions (e.g., Bonamici et al., 2015; Corvò et al., 2023). Whereas Bonamici et al. (2015) did not describe the twins in further detail, the twins recorded by Corvò et al. (2023) are characterized by the same disorientation axis of [102] and disorientation angle of 74°, but the twin planes were not specified. The observation that only in the Silvretta, pseudotachylyte-bearing fault rocks exhibit titanite twin planes close to $\{\bar{1}\bar{1}2\}$ in addition to those with {221} twin planes (Fig. 6a–d), is assumed to be related to higher stresses compared to the Sesia mylonites. Furthermore, the observed twin density is higher for the Silvretta (2.5 μm^{-1}) compared to the Sesia (0.5 μm^{-1}), which likewise implies higher differential stresses. The proportional dependence of the twin density on stress is characteristic of mechanical twinning (e.g., Christian and Mahajan 1995), which is, however, not quantitatively calibrated for titanite.

Similar fine-lamellar mechanical twins in ilmenite parallel to $\{10\bar{1}1\}$ characterized by a disorientation axis $< 1\bar{1}0\bar{1} >$ and disorientation angle of approximately 69° as described here (Fig. 6a, e) have also been observed in shocked Vredefort gneisses (Dellefant et al., 2022) as well as from shock experiments and lunar samples (Minkin and Chao, 1971;

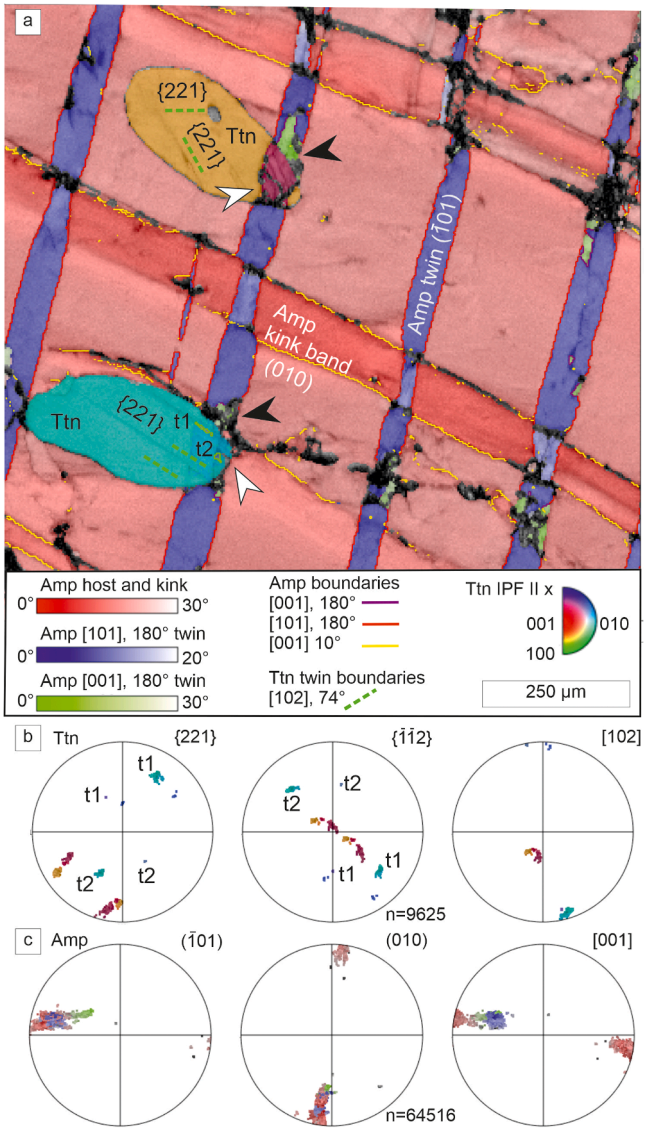

Fig. 7. EBSD map of twinned amphibole (Amp) with titanite (Ttn) inclusions, Silvretta pseudotachylyte-bearing fault rock, sample LB22. (a) Inverse Pole Figure (IPF) color-coding with relative misorientation for amphibole host (red), twin (blue, twin boundaries in red, low-angle grain boundaries in yellow) and included titanite with twin boundaries (dashed green lines). Titanite is affected by amphibole twins (white arrows), and kink bands are affected by titanite inclusion (black arrow). (b, c) Pole figures for titanite (Ttn) and amphibole (Amp), respectively.

Sclar et al., 1973). To our knowledge, ilmenite twins parallel $\{10\bar{1}1\}$ have not been described in tectonic fault rocks before.

The rare occurrence of twinned titanite in fault rocks and the common occurrence in impact breccias are in accordance with a relatively high CRSS for twinning in titanite of 130 MPa (Borg and Heard, 1972). As twinning requires a CRSS on the twin plane in the shear direction, twinning is dependent on the orientation of the crystal to the external stress field, following the Schmid formular:

$$\tau_{res} = \sigma_d \cdot \cos\gamma \cdot \cos\theta,$$

where τ_{res} is the resolved shear stress, σ_d is the differential stress, γ is the angle of the plane normal and θ the angle of the glide direction to the maximum principal stress direction, $\cos\gamma \cdot \cos\theta$ is known as Schmid factor, which has a maximum at 0.5. Thus, a differential stress of $>$ 260 MPa is required in the most suitable orientation of the titanite to the external stress field. The orientation distribution of twinned and not-twinned jadeite in the Sesia mylonites was used applying the Schmid formular to indicate the orientation of the maximum principal stress direction by Trepmann and Stöckhert (2001). The study reported that stresses at sample scale are relatively uniform but vary on a scale of hundreds of meters. The limitations to estimate the orientation of the principal stress directions by the orientation distribution of twins further include: twinned crystals may rotate during subsequent creep, the stress-strain field is heterogeneous dependening on surrounding minerals with different physical properties, as indicated by the "indentation microstructures" presented here (Figs. 2–4, 6–8, S1b, c), the twin plane may be oriented at a low angle to the thin section plane such that twins may not be visible although being present.

The recorded orientation variance of titanite twin planes of 2–90° and 3–76° to the foliation of the Sesia mylonites and Silvretta gneisses, respectively, may therefore be explained by high differential stresses exceeding the required 260 MPa for the most suitable orientation of the titanite to the stress field, which allows twinning also in orientations with relatively low resolved shear stress on the twin plane in the shear direction. Yet, a heterogeneous stress-strain field is likely and a later rotation of the crystals during subsequent modification as well as an observation bias cannot be excluded. Consistent to the differential stress in excess of 260 MPa indicated by the twinned titanite, differential stresses on the order of 0.5 GPa have been inferred by the jadeite twin paleopiezometers in the Sesia mylonites (Fig. 1b; Trepmann and Stöckhert, 2001) and by the presence of amphibole twins in the pseudotachylyte-bearing Silvretta gneisses (Figs. 5a, 6, 7; Brückner and Trepmann, 2021). Jadeite and amphibole have high CRSS of 150 ± 50 MPa (Orzol et al., 2003) and 200–400 MPa (Rooney et al., 1970), respectively.

Stresses of hundreds of MPa at greenschist facies conditions indicated in heterogeneous microstructures with partly recrystallized quartz requires rapid stress-loading and -unloading rates, consistent with coseismic off-fault deformation at and below hypocentral depths (Brückner et al., 2024; Küster and Stöckhert, 1999; Trepmann and Stöckhert, 2001, Trepmann et al., 2017; Trepmann et al., 2019). If stresses on that order had prevailed over a longer period at greenschist facies conditions, the quartz microstructure would be expected to show more intense dynamic recrystallization, as discussed for the Sesia zone mylonites by Trepmann and Stöckhert (2001) and the Silvretta gneisses by Brückner and Trepmann (2021).

5.2. *Comminution and cataclasis at an early stage of accelerated creep*

For frictional melting, preceding brittle fragmentation is required, which increases the surface area and lowers the thermal conductivity (e.g., Magloughlin and Spray, 1992; Sibson, 1975; Spray, 1995, 1987). The propagation of pseudotachylytic veins requires further brittle deformation. Pseudotachylytic veins can form at the same time distributed within the damage zone. Upon propagating through the host rock, they can mutually cross-cut each other without representing different generations (e.g., Brückner et al., 2024; Rowe et al., 2018). The deflection of fine-lamellar twins in titanite with an increased misorientation adjacent to pseudotachylytic veins (Fig. 8a–c) indicates that twinning predated the cross-cutting of pseudotachylytic veins. This is consistent with the missing systematic relationship between the occurrences and density of twins with the distance to pseudotachylytic veins. That amphibole, in contrast to titanite, is comminuted and integrated into the pseudotachylytic vein (Fig. 8a–c), confirms that amphibole is more prone to fusion and frictional melting than titanite at the given conditions. Titanite, zircon and apatite show fracture patterns that are characterized by more or less isometric clasts with low aspect ratio and missing shear offset (Fig. 8). Fracture patterns without shear offset and isometric clasts are commonly described during seismic rupturing (e.g., Austrheim et al., 2017; Campbell and Menegon, 2022; Reches and Dewers, 2005; Toffol et al., 2024).

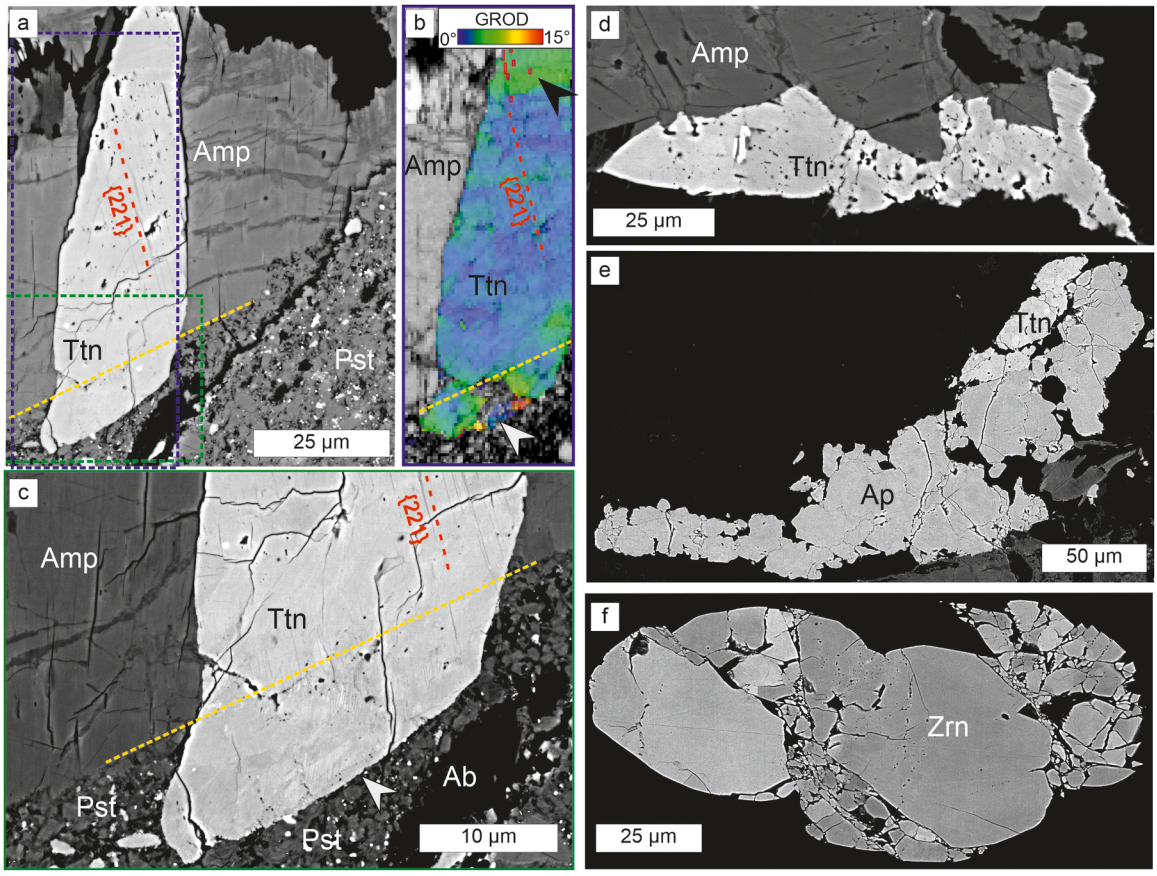

Fig. 8. Brittle deformation, Silvretta pseudotachylyte-bearing fault rock, sample LB21. (a) Amphibole (Amp) and titanite (Ttn) adjacent to pseudotachylytic vein (Pst) with albite (Ab) clasts and (b) corresponding GROD angle EBSD map of titanite (blue rectangle). Note a few fine twin lamellae (red dashed line) that are only locally detectable by EBSD (black arrow), as well as unindexed area marked by the white arrow. (c) Close-up BSE image marked by green rectangle in (a). The yellow dashed line marks the titanite affected by the pseudotachylyte, the white arrow points to the same area as in (b). (d) Twinned and fractured amphibole (Amp) with fragments indenting into fragmented titanite (Ttn). (e) Fragmented apatite (Ap) and titanite (Ttn). (f) Fragmented zircon (Zrn).

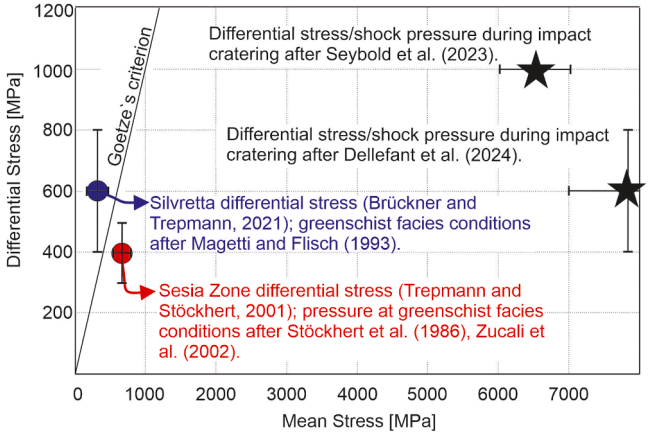

Fig. 9. Differential stress plotted against confining pressure. Conditions for Sesia zone mylonites, Silvretta fault rocks and impactites are plotted in relation to Goetze's criterion, see text for discussion.

In contrast, in the Sesia zone mylonites, systematic cataclasis with sets of subparallel fractures at angles of 60–80° to the mylonitic foliation occurs in titanite, jadeite, garnet, apatite and zircon in the mylonites (Figs. 1a, c, 3e, 4a, b). As titanite twin lamellae can continue across separated titanite fragments (Fig. 3e), this cataclasis is interpreted to have formed after twinning. The bending of the twin planes also indicates that twinning occurred before the local indentation of garnet and zircon (red arrows Figs. 2a, 3e). The systematic orientation of the fractures at angles of 60–80° to the mylonitic foliation, suggests that cataclasis occurred associated with the creeping quartz matrix at already relaxing stresses. The transient peak stress conditions during faulting

Table 1
Overview of microstructural characteristics of different deformation episodes distinguished by different stress/strain-rate conditions at approximately constant pressure and temperature.

	Sesia mylonites	Silvretta pseudotachylytes
High-stress crystal plasticity at several hundred MPa.	° Twinning of titanite (Figs. 2, 3), jadeite (Fig. 1b) and rutile (Fig. S1b, c). ° Quartz dislocation glide → deformation lamellae and microcracks (Figs. 1c, 2a, 4).	° Twinning of titanite, ilmenite and amphibole (Figs. 5–8). ° Fragmentation of zircon, apatite, titanite → isometric fragments and comminution of amphibole and fusion → pseudotachylyte formation (Fig. 8).
Subsequent modification at decreasing stresses.	° Dislocation creep of quartz and associated cataclasis with sets of subparallel fractures in titanite garnet, jadeite, zircon (Figs. 1c, 2a, 3, 4). ° Precipitation of albite and quartz from the pore fluid along opening fractures (Figs. 3e, 4).	° No subsequent dislocation creep of quartz and no similar cataclasis (sets of subparallel fractures), instead: tensile cracking and healing with growth of quartz at low stress: cleavage fractures in quartz (Brückner et al., 2024).

recorded in both settings are close to conditions reached in deformation experiments with several hundred MPa differential stress and strain rates probably on the order of 10^{-5} s^{-1} or even higher, where titanite, jadeite, and amphibole deform by twinning (e.g., Borg and Heard, 1972; Orzol et al., 2003; Rooney et al., 1970). At these deformation conditions at the given pressure-temperature conditions (Fig. 9), quartz dislocation climb is not effective and thus does not allow for recovery, which leads to strain hardening (e.g., Hobbs, 1968; Trepmann et al., 2007), where at subsequently decreasing stresses, quartz deforms by dislocation creep (Trepmann and Stöckhert, 2003). Fracturing of rigid inclusions embedded in a ductile matrix has been reported in several geological studies (e.g., Hentschel et al., 2022; Ji et al., 1997; Trepmann and Stöckhert, 2002) and can be explained by stress loading upon the creeping matrix to their brittle yield strength (e.g., Chen et al., 2023; Le et al., 2005). The observation that dislocation creep of quartz occurred after the high-stress deformation during accelerated creep (Figs. 1c, 2a, 3a, b) is consistent with the findings from Trepmann and Stöckhert (2003). Upon stress relaxation after fracturing, the fragments slightly open with albite and/or quartz precipitate from the pore fluid (Figs. 3e, 4), as discussed for the similar fracture pattern of garnets (Trepmann and Stöckhert, 2002).

5.3. Comparison of Sesia mylonites and Silvretta pseudotachylytes

The recorded high stresses at greenschist facies conditions in association with the heterogeneity of the microstructures in both fault rocks reflect transient stress conditions. In both tectonic settings, twinning at high stress occurred at an early stage before cross-cutting of pseudotachylytic veins in the Silvretta (Fig. 8) and before cataclasis in the Sesia zone mylonites (Figs. 2a, 3a, b, e). That twinning is influencing deformation in the surrounding quartz is documented for example by deformation lamellae in quartz at the contact to twinned titanite (Fig. 4). Twinning in amphibole transferred stress and strain into titanite inclusions and vice versa (Fig. 7). In general, the "indentation microstructures" (Figs. 2–4, 6–8, S1b, c) record the influence of varying mechanical properties of neighboring minerals and heterogeneous stress-strain conditions during deformation, as characteristic for transient high stress conditions.

Yet, the history after twinning is quite different with distributed pseudotachylyte formation in the Silvretta and cataclasis upon accelerated creep in the Sesia zone mylonites. Brittle strength is predicted to be higher for thrusting than for strike-slip faulting, which controls the maximum expected differential stresses at the base of the seismogenic zone (e.g., Scholz, 2002). Thus, the maximum differential stress can be expected in the Silvretta fault rocks to have been higher compared to the Sesia strike-slip tectonic setting. This is consistent with our observations of different titanite twin planes and higher twin densities in the Silvretta fault rocks compared to the Sesia zone mylonites with 2.5 μm^{-1} and 0.5 μm^{-1}, respectively (compare Fig. 2c, Fig. 6b–d). Higher transient stresses and strain rates are also consistent with the frequent occurrence of pseudotachylytes in the Silvretta fault rocks.

Yet, subsequent accelerated creep is only recorded in the Sesia zone mylonites by the cataclastic deformation of titanite and dislocation creep of quartz (Figs. 2, 3, 4). The quartz microfabrics of the pristine pseudotachylyte-bearing gneisses in direct association with amphibole-rich layers (Fig. 1d) that formed at greenschist facies conditions are described in detail by Brückner et al. (2023). They do not show evidence of dislocation creep after pseudotachylyte formation. On the contrary, quartz has been reported to show quasi-static recrystallization along the damage zone of cleavage cracks, which formed upon tensile cracking after pseudotachylyte formation (Brückner et al., 2024). The missing evidence of creep and instead the evidence of quasi-static recrystallization have been taken to indicate fast stress relaxation. The faster stress relaxation for the Silvretta fault rocks compared to the Sesia mylonites is interpreted to be controlled by the lower mean stress conditions favoring brittle deformation and the more efficient stress attenuation upon formation of pseudotachylytes (Fig. 9). These major differences in the record of the Sesia mylonites and the Silvretta fault rocks demonstrate how high-stress crystal plasticity controls the stress/strain history during coseismic loading and postseismic/interseismic creep at or just below hypocentral depths.

In addition, the distance to the seismic active rupture, which controls the stress/strain-rate conditions, has to be considered (Brückner et al., 2023; Nüchter et al., 2013). Both fault rocks, the Sesia zone mylonites as well as the pseudotachylyte-bearing Silvretta gneisses, represent off-fault damage but at different distances to the seismically active major rupture plane with stress perturbations related to seismic rupturing (e.g., Dielforder et al., 2023; Ellis and Stöckhert, 2004; Ellis et al., 2006; Nüchter and Ellis, 2011; Reches and Dewers, 2005; Ulrich et al., 2019). The Sesia zone mylonites represent a transient high-stress deformation episode at temperatures of about 350 ± 50 °C (Küster and Stöckhert, 1999; Trepmann and Stöckhert, 2003, 2002, 2001). The rocks were below 280 ± 30 °C already at ca. 35 Ma as indicated by fission track ages of zircon and apatite (Hurford et al., 1991). Most probably, the high-stress crystal plasticity is associated with the uplift of the Sesia Zone by several tens of kilometers with respect to the adjacent South Alpine basement (Ivrea Zone) in Oligocene and Miocene times along a precursor fault of the Insubric Fault (Küster and Stöckhert, 1999; Trepmann and Stöckhert, 2003). The seismogenic zone originally overlying the mylonite-bearing horizon of the Sesia zone exposed today is not preserved. Therefore, no further information on the geometry and size of the damage zone is feasible.

The pseudotachylyte-bearing gneisses at the base of the Silvretta nappe represent the detachment of the nappe before its thrusting over the Penninic units (Brückner et al., 2023; Koch and Masch, 1992; Laubscher, 1983), where the footwall of the fault has not been preserved. The pseudotachylytes occur in an area of at least 100 km^2 and up to 900 m above today's contact with the overthrusted Penninic units (Schmutz, 1995).

5.4. High-stress crystal plasticity during hypervelocity meteorite impact

Conditions of transient high differential stresses on the order of 0.5 GPa and mean stresses high enough to prevent brittle deformation are realized not only coseismically at or just below the seismogenic zone but also during hypervelocity impact at low to moderate shock conditions (Fig. 9, Melosh, 1989; Trepmann, 2008; Rae et al., 2021; Seybold et al., 2023; Dellefant et al., 2024a). Under these conditions, rock-forming minerals can undergo high-stress crystal plasticity, which is especially recorded by mechanical twinning of minerals characterized by a high CRSS, such as amphibole (Dellefant et al., 2024a) and titanite (Timms et al., 2019). At higher shock conditions, the loading to and unloading from higher mean stresses favor phase transformations, including the formation of diaplectic glass (e.g., Dellefant et al. 2024b, Stöffler et al., 2018 and references therein). Maskelynite (diaplectic glass of feldspar) has, for example, been found associated with [101] amphibole twins (Dellefant et al., 2024a). The stress relaxation after shock is extremely fast (on the order of seconds, e.g., Melosh, 1989), as indicated by numerical models (e.g., Rae et al., 2021). Subsequent modification is generally low compared to fault rocks exhumed from the base of the seismogenic zone. The study of high-stress crystal plasticity recorded by impact breccias is very valuable to detect and identify transient high-stress imprints in fault rocks that are usually more (Sesia zone mylonites) or less (Silvretta fault rocks) modified upon subsequent creep during the prolonged thermal history before exhumation.

6. Conclusions

High-stress microstructures in fault rocks and especially mechanical twins in minerals with high CRSS allow the identification and recognition of transient high-stress events, even if the microfabric is modified during subsequent creep at low stresses, beyond the presence of

pseudotachylytes.

The comparison of fault rocks from different tectonic settings formed at the same temperature conditions of 350 ± 50 °C can be summarized as follows:

- Mechanical twinned titanite with ⟨110⟩ glide direction indicates transient high differential stresses on the order of several hundred MPa for both tectonic settings.
- Twinning at high stress occurred before cross-cutting of pseudotachylytic veins in the Silvretta gneisses and cataclasis in the Sesia zone mylonites.
- Higher differential stresses and strain rates for the Silvretta fault rocks are indicated by a higher twin density and various twin planes for titanite, the presence of fine-lamellar mechanical twins in ilmenite parallel to $\{10\bar{1}1\}$ and a disorientation axis $< 1\bar{1}0\bar{1} >$ as well as the presence of pseudotachylytes.
- The higher stresses and strain rates are consistent with the thrust fault setting in the Silvretta as opposed to the strike-slip tectonic setting in the Sesia zone, as well as a larger distance to the seismic active rupture and higher mean stresses for the Sesia mylonites.
- In the Sesia mylonites, cataclasis characterized by a regular fracture pattern with subparallel intragranular fractures formed after twinning and upon stress relaxation during creep of the surrounding quartz matrix.
- Significantly faster stress relaxation rates in the Silvretta fault rocks are indicated by missing evidence for subsequent creep, as well as missing similar fracture patterns with sets of parallel fractures and are explained by the lower mean stresses favoring pseudotachylyte formation with more efficient stress relaxation rates.

The similarities of the high-stress crystal plasticity in both settings (differential stresses on the order of several hundred MPa up to GPa) as well as the differences (pseudotachylyte formation in the Silvretta fault rocks and creep at more slowly decreasing stresses in the Sesia zone mylonites), demonstrate the importance of deformation at transient high stresses for the subsequent stress-strain history. Our study highlights the need to consider episodic deformation at transient peak stress to develop more realistic fault models.

CRediT authorship contribution statement

Claudia A. Trepmann: Writing – review & editing, Writing – original draft, Visualization, Validation, Supervision, Software, Resources, Project administration, Methodology, Investigation, Funding acquisition, Formal analysis, Data curation, Conceptualization. **Lisa M. Beiers:** Writing – review & editing, Visualization, Validation, Investigation. **Fabian Dellefant:** Writing – review & editing, Validation, Investigation.

Declaration of competing interest

The authors declare that they have no known competing financial interests or personal relationships that could have appeared to influence the work reported in this paper.

Acknowledgements

This study was funded by the German Research Foundation (DFG Grant No TR 534/8–1). We are grateful to three anonymous referees for their constructive and thorough reviews, as well as for the editorial handling of Alexander Webb, which helped to improve the manuscript.

Supplementary materials

Supplementary material associated with this article can be found, in the online version, at doi:10.1016/j.epsl.2025.119741.

Data availability

Data will be made available on request.

References

Anderson, E.K., Song, W.J., Johnson, S.E., Cruz-Uribe, A.M., 2021. Mica kink-band geometry as an indicator of coseismic dynamic loading. Earth Planet. Sci. Lett. 567, 117000. https://doi.org/10.1016/j.epsl.2021.117000.

Austrheim, H., Dunkel, K.G., Plümper, O., Ildefonse, B., Liu, Y., Jamtveit, B., 2017. Fragmentation of wall rock garnets during deep crustal earthquakes. Sci. Adv. 3 (2), e1602067. https://doi.org/10.1126/sciadv.1602067.

Bachmann, R., Oncken, O., Glodny, J., Seifert, W., Georgieva, V., Sudo, M., 2009. Exposed plate interface in the European Alps reveals fabric styles and gradients related to an ancient seismogenic coupling zone. J. Geophys. Res. Solid Earth 114, B05402. https://doi.org/10.1029/2008JB005927.

Bonamici, C.E., Fanning, C.M., Kozdon, R., Fournelle, J.H., Valley, J.W., 2015. Combined oxygen-isotope and U-Pb zoning studies of titanite: new criteria for age preservation. Chem. Geol. 398, 70–84. https://doi.org/10.1016/j.chemgeo.2015.02.002.

Borg, I.Y., 1970. Mechanical < 110 >twinning in shocked sphene. Am. Mineral. 55, 1876–1888.

Borg, I.Y., Heard, H.C., 1972. Mechanical twinning in sphene at 8 kbar, 25° to 500 °C. pp. 585–592. https://doi.org/10.1130/MEM132-p585.

Brückner, L.M., Dellefant, F., Trepmann, C.A., 2024. Quartz cleavage fracturing and subsequent recrystallization along the damage zone recording fast stress unloading. J. Struct. Geol. 178, 105008. https://doi.org/10.1016/j.jsg.2023.105008.

Brückner, L.M., Trepmann, C.A., 2021. Stresses during pseudotachylyte formation - evidence from deformed amphibole and quartz in fault rocks from the Silvretta basal thrust (Austria). Tectonophysics 817, 229046. https://doi.org/10.1016/j.tecto.2021.229046.

Brückner, L.M., Trepmann, C.A., Kaliwoda, M., 2023. Rheology dependent on the distance to the propagating thrust tip—(Ultra-)Mylonites and pseudotachylytes of the Silvretta Basal Thrust. Tectonics 42, e2023TC008010. https://doi.org/10.1029/2023TC008010.

Campbell, L.R., Menegon, L., 2022. High stress deformation and short-term thermal pulse preserved in pyroxene microstructures from exhumed lower crustal seismogenic faults (Lofoten, Norway). J. Geophys. Res. Solid. Earth. 127, e2021JB023616. https://doi.org/10.1029/2021JB023616.

Chen, T., Ji, S., Tang, C., Foulger, G.R., Gong, B., 2023. Fracture spacings of fiber inclusions in a ductile geological matrix and development of microboudins: 3D numerical modeling. J. Struct. Geol. 174, 104920. https://doi.org/10.1016/j.jsg.2023.104920.

Christian, J.W., Mahajan, S., 1995. Deformation twinning. Prog. Mater. Sci. 39, 1–157. https://doi.org/10.1016/0079-6425(94)00007-7.

Corvò, S., Maino, M., Piazolo, S., Kylander-Clark, A.R.C., Orlando, A., Seno, S., Langone, A., 2023. Crystal plasticity and fluid availability govern the ability of titanite to record the age of deformation. Earth Planet. Sci. Lett. 620, 118349. https://doi.org/10.1016/j.epsl.2023.118349.

Dellefant, F., Seybold, L., Trepmann, C.A., Gilder, S.A., Sleptsova, I.V., Hölzl, S., Kaliwoda, M., 2024a. Emplacement of shocked basement clasts during crater excavation in the Ries impact structure. Int. J. Earth Sci. 113, 951–971. https://doi.org/10.1007/s00531-024-02403-z.

Dellefant, F., Trepmann, C.A., Gilder, S.A., Sleptsova, I.V., Kaliwoda, M., Weiss, B.P., 2022. Ilmenite and magnetite microfabrics in shocked gneisses from the Vredefort impact structure, South Africa. Contrib. Mineral. Petrol. 177, 88. https://doi.org/10.1007/s00410-022-01950-5.

Dellefant, F., Trepmann, C.A., Schmahl, W.W., Gilder, S.A., Sleptsova, I.V., Kaliwoda, M., 2024b. Ilmenite phase transformations in suevite from the Ries impact structure (Germany) record evolution in pressure, temperature, and oxygen fugacity conditions. Am. Mineral. 109, 1005–1023. https://doi.org/10.2138/am-2023-8985.

Dielforder, A., Bocchini, G.M., Kemna, K., Hampel, A., Harrington, R.M., Oncken, O., 2023. Megathrust stress drop as trigger of aftershock seismicity: insights from the 2011 Tohoku Earthquake, Japan. Geophys. Res. Lett., 50, e2022GL101320. https://doi.org/10.1029/2022GL101320.

Ellis, S., Beavan, J., Eberhart-Phillips, D., Stöckhert, B., 2006. Simplified models of the Alpine Fault seismic cycle: stress transfer in the mid-crust. Geophys. J. Int. 166, 386–402. https://doi.org/10.1111/j.1365-246X.2006.02917.x.

Ellis, S., Stöckhert, B., 2004. Elevated stresses and creep rates beneath the brittle-ductile transition caused by seismic faulting in the upper crust. J. Geophys. Res. Solid. Earth. 109, B05407, doi:10.1029/2003JB002744.

Frost, H.J., Ashby, M.F., 1982. Deformation-mechanism maps: the Plasticity and Creep of Metals and Ceramics. first ed. Pergamon Press, Oxford.

Hentschel, F., Janots, E., Magnin, V., Brückner, L.M., Trepmann, C.A., 2022. Transient deformation and long-term tectonic activity in the Eastern Alps recorded by mylonitic pegmatites. J. Struct. Geol. 155, 104507. https://doi.org/10.1016/j.jsg.2021.104507.

Hobbs, B.E., 1968. Recrystallization of single crystals of quartz. Tectonophysics 6, 353–401.

Hurford, A.J., Hunziker, J.C., Stöckhert, B., 1991. Constraints on the late thermotectonic evolution of the western Alps: eVidence for episodic rapid uplift. Tectonics 10, 758–769. https://doi.org/10.1029/91TC00167.

Ji, S., Zhao, P., Saruwatari, K., 1997. Fracturing of garnet crystals in anisotropic metamorphic rocks during uplift. J. Struct. Geol. 19, 603–620. https://doi.org/10.1016/S0191-8141(97)00006-0.

Kameyama, M., Yuen, D.A., Karato, S.-I., 1999. Thermal-mechanical effects of low-temperature plasticity (the Peierls mechanism) on the deformation of a viscoelastic shear zone. Earth Planet. Sci. Lett. 168, 159–172. https://doi.org/10.1016/S0012-821X(99)00040-0.

Koch, N., Masch, L., 1992. Formation of Alpine mylonites and pseudotachylytes at the base of the Silvretta nappe, Eastern Alps. Tectonophysics 204, 289–306. https://doi.org/10.1016/0040-1951(92)90313-U.

Küster, M., Stöckhert, B., 1999. High differential stress and sublithostatic pore fluid pressure in the ductile regime - microstructural evidence for short-term post-seismic creep in the Sesia Zone, Western Alps. Tectonophysics 303, 263–277. https://doi.org/10.1016/S0040-1951(98)00256-X.

Laubscher, H.P., 1983. Detachment, shear, and compression in the central Alps. Geol. Soc. Am. 158, 191–211.

Le, K.C., Korobeinik, M., Hackl, K., 2005. Estimation of crack density due to fragmentation of brittle ellipsoidal inhomogeneities embedded in a ductile matrix. Arch. Appl. Mech. 74, 439–448. https://doi.org/10.1007/s00419-004-0367-0.

Maggetti, M., Flisch, M., 1993. Evolution of the silvretta nappe. In: Raumer, J.F., Neubaue, F. (Eds.), Pre-Mesozoic Geology in the Alps. Springer Berlin Heidelberg, Berlin, Heidelberg, pp. 469–484.

Magloughlin, J.F., Spray, J.G., 1992. Frictional melting processes and products in geological materials: introduction and discussion. Tectonophysics 204, 197–204. https://doi.org/10.1016/0040-1951(92)90307-R.

McGregor, M., Erickson, T.M., Spray, J.G., Whitehouse, M.J., 2021. High-resolution EBSD and SIMS U–Pb geochronology of zircon, titanite, and apatite: insights from the Lac La Moinerie impact structure, Canada. Contrib. Mineral. Petrol. 176, 76. https://doi.org/10.1007/s00410-021-01828-y.

Melosh, H.J., 1989. Impact Cratering: a Geological Process. Oxford Monographs on Geology and Geophysics #11. Oxford University Press, New York.

Minkin, J.A., Chao, E.C.T., 1971. Single crystal X-ray investigation of deformation in terrestrial and lunar ilmenite. Proc. Lunar Sci. Conf. 2, 237–246.

Müller, W.F., Franz, G., 2004. Unusual deformation microstructures in garnet, titanite and clinozoisite from an eclogite of the Lower Schist Cover, Tauern Window, Austria. Eur. J. Mineral. 16, 939–944. https://doi.org/10.1127/0935-1221/2004/0016-0939.

Nüchter, J.-A., Ellis, S., 2011. Mid-crustal controls on episodic stress-field rotation around major reverse, normal and strike-slip faults. In: Fagereng, Å., Toy, V.G., Rowland, J.V. (Eds.), Geology of the Earthquake Source: A Volume in Honour of Rick Sibson, Geological Society, Geology of the Earthquake Source: A Volume in Honour of Rick Sibson, Geological Society, 359. Special Publications, London, pp. p187–p201. https://doi.org/10.1144/SP359.11, 2011v.

Nüchter, J.A., Wassmann, S., Stöckhert, B., 2013. Cyclic ductile and brittle deformation related to coseismic thrust fault propagation: structural record at the base of a basement nappe (Preveli, Crete). Tectonics 32 (5), 1272–1293. https://doi.org/10.1002/tect.20079.

Orzol, J., Trepmann, C.A., Stöckhert, B., Shi, G., 2003. Critical shear stress for mechanical twinning of jadeite—An experimental study. Tectonophysics 372, 135–145. https://doi.org/10.1016/S0040-1951(03)00242-7.

Papapavlou, K., Darling, J.R., Moser, D.E., Barker, I.R., White, L.F., Lightfoot, P.C., Storey, C.D., Dunlop, J., 2018. U–Pb isotopic dating of titanite microstructures: potential implications for the chronology and identification of large impact structures. Contrib. Mineral. Petrol. 173, 82. https://doi.org/10.1007/s00410-018-1511-0.

Pittarello, L., Levi, N., Wegner, W., Stehlik, H., 2022. The pseudotachylytes at the base of the Silvretta nappe: a newly discovered recent generation and the tectonomometamophic evolution of the Nappe. Tectonophysics 822, 229185. https://doi.org/10.1016/j.tecto.2021.229185.

Poelchau, M.H., Winkler, R., Kenkmann, T., Wirth, R., Luther, R., Schäfer, F., 2025. Extreme twin densities in calcite - A shock indicator. Geology 53, 279–283. https://doi.org/10.1130/G52795.1.

Rae, A.S.P., Poelchau, M.H., Kenkmann, T., 2021. Stress and strain during shock metamorphism. Icarus 370, 114687. https://doi.org/10.1016/j.icarus.2021.114687.

Reches, Z., Dewers, T., 2005. Gouge formation by dynamic pulverization during earthquake rupture. Earth Planet. Sci. Lett. 235, 361–374. https://doi.org/10.1016/j.epsl.2005.04.009.

Rooney, T.P., Riecker, R.E., Ross, M., 1970. Deformation twins in Hornblende. Science (1979) 169, 173–175. https://doi.org/10.1126/science.169.3941.173.

Rowe, C.D., Ross, C., Swanson, M.T., Pollock, S., Backeberg, N.R., Barshi, N.A., Bate, C. E., Carruthers, S., Coulson, S., Dascher-Cousineau, K., Harrichhausen, N., Peña Castro, A.F., Nisbet, H., Rakoczy, P., Scibek, J., Smith, H., Tarling, M.S., Timofeev, A., Young, E., 2018. Geometric complexity of earthquake rupture surfaces preserved in pseudotachylyte networks. J. Geophys. Res. Solid Earth 123, 7998–8015. https://doi.org/10.1029/2018JB016192.

Schmid, S.M., Aebli, H.R., Heller, F., Zingg, A., 1989. The role of the Periadriatic Line in the tectonic evolution of the Alps. Geological Society 45, 153–171. https://doi.org/10.1144/GSL.SP.1989.045.01.08.

Schmid, S.M., Fügenschuh, B., Kissling, E., Schuster, R., 2004. Tectonic map and overall architecture of the Alpine orogen. Eclogae Geol. Helv. 97, 93–117. 10.1007/s00015-004-1113-x.

Schmutz, H.-U., 1995. Geologische Untersuchungen im SW-Teil Des Unterengadiner Fensters: Teil II, Die makroskopische Geometrie der Pseudotachylite in Der Silvretta-Decke am NW-Rand Des Unterengadiner Fensters, Beiträge zur geologischen Karte der Schweiz, 1420-2875 n.F., 166. Baumgartner Druck AG, Burgdorf.

Scholz, C.H., 2002. The Mechanics of Earthquakes and Faulting, 2nd ed. Cambridge University Press, New York.

Sclar, C.B., Bauer, J.F., Pickart, S.J., Alperin, H.A., 1973. Shock effects in experimentally shocked terrestrial ilmenite, lunar ilmenite of rock fragments in 1–10 mm fines (10085,19), and lunar rock 60015,127. Proc. Fourth Lunar Sci. Conf. 4, 841–859.

Seybold, L., Trepmann, C.A., Hölzl, S., Pollok, K., Langenhorst, F., Dellefant, F., Kaliwoda, M., 2023. Twinned calcite as an indicator of high differential stresses and low shock pressure conditions during impact cratering. Meteorit. Planet. Sci. 58, 1287–1305. https://doi.org/10.1111/maps.14056.

Sibson, R.H., 1975. Generation of pseudotachylyte by ancient seismic faulting. Geophys. J. R. Astron. Soc. 43, 775–794. https://doi.org/10.1111/j.1365-246X.1975.tb06195.x.

Spray, J.G., 1987. Artificial generation of pseudotachylyte using friction welding apparatus: simulation of melting on a fault plane. J. Struct. Geol. 9, 49-60.

Spray, J.G., 1995. Pseudotachylyte controversy: fact or friction? Geology 23 1119–1122. 10.1130/0091-7613(1995)023<1119:PCFOF>2.3.CO;2.

Stöckhert, B., Jäger, E., Voll, G., 1986. K - Ar age Determinations On Phengites from the Internal Part of the Sesia Zone, 92. Contrib. Mineral. Petrol., Western Alps, Italy, pp. 456–470. https://doi.org/10.1007/BF00374428.

Stöffler, D., Hamann, C., Metzler, K., 2018. Shock metamorphism of planetary silicate rocks and sediments: proposal for an updated classification system. Meteorit. Planet. Sci. 53, 5–49. https://doi.org/10.1111/maps.12912.

Thöni, M., 1988. Rb-Sr isotopic resetting in mylonites and pseudotachylites: implications for the detachment and thrusting of the Austroalpine basement nappes in the Eastern Alps. Jahrb. Geol. Bundesanst. 131, 169–201.

Timms, N.E., Pearce, M.A., Erickson, T.M., Cavosie, A.J., Rae, A.S.P., Wheeler, J., Wittmann, A., Ferrière, L., Poelchau, M.H., Tomioka, N., Collins, G.S., Gulick, S.P.S., Rasmussen, C., Morgan, J.V., 2019. New shock microstructures in titanite (CaTiSiO5) from the peak ring of the Chicxulub impact structure, Mexico. Contrib. Mineral. Petrol. 174, 38. https://doi.org/10.1007/s00410-019-1565-7.

Toffol, G., Pennacchioni, G., Menegon, L., Wallis, D., Faccenda, M., Camacho, A., Bestmann, M., 2024. On-fault earthquake energy density partitioning from shocked garnet in an exhumed seismic midcrustal fault. Sci. Adv. 10, eadi8533. https://doi.org/10.1126/sciadv.adi8533.

Trepmann, C.A., 2008. Shock effects in quartz: compression versus shear deformation — An example from the Rochechouart impact structure, France. Earth Planet. Sci. Lett. 267, 322–332. https://doi.org/10.1016/j.epsl.2007.11.035.

Trepmann, C.A., Hsu, C., Hentschel, F., Döhler, K., Schneider, C., Wichmann, V., 2017. Recrystallization of quartz after low-temperature plasticity – The record of stress relaxation below the seismogenic zone. J. Struct. Geol. 95, 77–92. https://doi.org/10.1016/j.jsg.2016.12.004.

Trepmann, C.A., Seybold, L., Janots, E., 2019. Deformation at low and high stress-loading rates. Geosci. Front. 10, 43–54. https://doi.org/10.1016/j.gsf.2018.05.002.

Trepmann, C.A., Stöckhert, B., 2001. Mechanical twinning of jadeite - an indication of synseismic loading beneath the brittle-plastic transition. Int. J. Earth Sci. 90, 4–13. https://doi.org/10.1007/s005310000165.

Trepmann, C.A., Stöckhert, B., 2002. Cataclastic deformation of garnet: a record of synseismic loading and postseismic creep. J. Struct. Geol. 24, 1845–1856. https://doi.org/10.1016/S0191-8141(02)00004-4.

Trepmann, C.A., Stöckhert, B., 2003. Quartz microstructures developed during non-steady state plastic flow at rapidly decaying stress and strain rate. J. Struct. Geol. 25, 2035–2051. https://doi.org/10.1016/S0191-8141(03)00073-7.

Trepmann, C.A., Stöckhert, B., Dorner, D., Moghadam, R.H., Küster, M., Röller, K., 2007. Simulating coseismic deformation of quartz in the middle crust and fabric evolution during postseismic stress relaxation — An experimental study. Tectonophysics 442, 83–104. https://doi.org/10.1016/j.tecto.2007.05.005.

Tsenn, M.C., Carter, N.L., 1987. Upper limits of power law creep of rocks. Tectonophysics 136, 1–26. https://doi.org/10.1016/0040-1951(87)90332-5.

Ulrich, T., Gabriel, A.-A., Ampuero, J.-P., Xu, W., 2019. Dynamic viability of the 2016 Mw 7.8 Kaikōura earthquake cascade on weak crustal faults. Nat. Commun. 10, 1213. https://doi.org/10.1038/s41467-019-09125-w.

Zucali, M., Spalla, M.I., 2011. Prograde lawsonite during the flow of continental crust in the Alpine subduction: strain vs. metamorphism partitioning, a field-analysis approach to infer tectonometamorphic evolutions (Sesia-Lanzo Zone, Western Italian Alps). J. Struct. Geol. 33, 381–398. https://doi.org/10.1016/j.jsg.2010.12.006.

Zucali, M., Spalla, M.I., Gosso, G., 2002. Strain partitioning and fabric evolution as a correlation tool: the example of the Eclogitic Micaschists Complex in the Sesia-Lanzo Zone (Monte Mucrone-Monte Mars, Western Alps, Italy). Schweiz. Mineral. Petrogr. Mitt. 82, 429–454.